

TARGETED DISRUPTION OF THE DOPAMINE D₂ AND D₃ RECEPTOR GENES LEADS TO DIFFERENT ALTERATIONS IN THE EXPRESSION OF STRIATAL CALBINDIN-D_{28k}

M.-Y. JUNG,* P. R. HOF† and C. SCHMAUSS*‡

*Department of Psychiatry/Neuroscience, Columbia University/New York State Psychiatric Institute, 1051 Riverside Drive, New York, NY 10032, U.S.A.

†Kastor Neurobiology of Aging Laboratories and Fishberg Research Center for Neurobiology, and Department of Geriatrics and Adult Development and Ophthalmology, Mount Sinai School of Medicine, New York, NY 10029, U.S.A.

Abstract—The present study used mice deficient for dopamine D₂ and D₃ receptors to test whether the expression of these two members of the D₂ class of receptors is essential for the normal expression of three markers that characterize the neurochemical differentiation of the striatum: the calcium-binding protein calbindin, tyrosine hydroxylase and acetylcholinesterase. Results from these experiments revealed that the expression of striatal tyrosine hydroxylase (the rate-limiting enzyme of dopamine synthesis) and acetylcholinesterase is unaffected even by the combined knockout of D₂ and D₃ receptors. However, D₂ and D₃ receptor knockouts differently affect the striatal expression of calbindin-D_{28k} immunoreactivity. Prominent changes in the cellular distribution of calbindin are detected in striatal neurons of D₂ mutant mice. Whereas calbindin immunolabeling of wild-type neurons is prominent in the nuclei and the cytoplasm of medium spiny neurons, in D₂ mutant mice, calbindin immunoreactivity is concentrated exclusively in the cytoplasmic rim of these neurons. Such changes in the cellular distribution of calbindin expression are not detected in mice lacking D₃ receptors. In these mutants, however, a lesser density of calbindin-immunoreactive neuropil is detected in the ventral portions of the striatum, i.e. in regions in which D₃ receptors are thought to be expressed at highest levels. Mice lacking both D₂ and D₃ receptors show both phenotypes.

The altered cellular distribution of calbindin in D₂ mutants is likely to have functional consequences for some of the Ca²⁺-mediated cellular functions. The topography of the decreased density of striatal calbindin immunoreactivity in D₃ mutants suggests a role for D₃ receptors in supporting the expression of striatal calbindin. The observation that mice lacking both D₂ and D₃ receptors show a combination of the D₂ and D₃ mutant phenotypes indicates that each of the different phenotypes detected in the single mutants is indeed related to the lack of the two different D₂-like receptor subtypes. © 2000 IBRO. Published by Elsevier Science Ltd.

Key words: D₂-like dopamine receptors, gene targeting, striatum, tyrosine hydroxylase, acetylcholinesterase, calbindin.

The four major neuronal systems of the brain that use dopamine (DA) as the principal neurotransmitter modulate locomotor behavior (nigrostriatal system), motivated behavior (mesolimbic system), learning and memory (mesocortical system), and the release of prolactin (tuberoinfundibular system). DA receptors, which are expressed in DA-synthesizing neurons and/or in the targets of the dopaminergic pathways, fall into two functionally distinct classes. The D₁ class of receptors (composed of the subtypes D₁ and D₅) couple to stimulatory subsets of heterotrimeric G-proteins and the D₂ class of receptors (composed of the subtypes D₂, D₃ and D₄) couple to inhibitory G-proteins.¹⁸ These receptors are the targets for drugs employed in the treatment of psychotic disorders and Parkinson's disease. Furthermore, psychostimulants such as cocaine and amphetamine indirectly activate these receptors.¹⁸

In the rodent, D₁, D₂ and D₃ receptor mRNAs are expressed as early as embryonic day 14.^{7,20,21} However, it is presently unclear whether the (differential) expression of these receptors

in the ganglionic eminence that is detected prior to the establishment of synaptic transmission is of functional relevance. In the developing and mature brain, D₁ and D₂ receptors are expressed at highest levels in the dorsal striatum, and the expression of D₃ receptors (which are also found in the striatum) is notably high in the nucleus accumbens of the ventral striatum.¹⁸ In recent years, several D₁, D₂ and D₃ receptor mutant mice have been generated by gene targeting via homologous recombination, and the constitutive knockout of these receptors led to viable homozygous mutants that develop receptor knockout-specific locomotor phenotypes.²² The most pronounced locomotor phenotype has been described for mice lacking D₂ receptors.^{3,13} These mutants show postural abnormalities and a progressive increase of locomotor hypoactivity during postnatal development, a phenotype that clearly differs from the reported normal⁹ or increased basal locomotor activity²⁴ of D₁ mutants. Moreover, although the D₂ mutant phenotype clearly differs from the corresponding locomotor phenotype observed in D₃ single mutants,^{1,13,25} mice lacking both D₂ and D₃ receptors develop a locomotor phenotype that is qualitatively similar but quantitatively more severe than that of D₂ single mutants.¹³

Like D₃ single mutants, mice lacking D₂ and D₂/D₃ receptors have normal tissue levels of DA.¹³ This suggests that an impaired functioning of anatomical structures that receive dopaminergic input underlies the development of the D₂-like locomotor phenotype. One key anatomical region is the

‡To whom correspondence should be addressed. Tel.: +1-212-543-6505; fax: +1-212-543-6017.

E-mail address: schmauss@neuron.cpmc.columbia.edu (C. Schmauss).

Abbreviations: AChE, acetylcholinesterase; CB, calbindin-D_{28k}; DA, dopamine; DAT, dopamine transporter; EGTA, ethyleneglycolbis(aminoethyl ether)tetra-acetate; IgG, immunoglobulin G; PBS, phosphate-buffered saline; PCR, polymerase chain reaction; RT, reverse transcriptase; TH, tyrosine hydroxylase.

neostriatum, a region involved in modulating motor behavior and known to express D₂ and D₃ receptors.¹⁸ One well-studied area is the neurochemical differentiation of the dorsal striatum, and the markers characteristic for the striatal patch (striosome) and matrix compartments, tyrosine hydroxylase (TH), acetylcholinesterase (AChE) and calbindin-D_{28k} (CB), proved very useful for structural studies on both the developing and the mature striatum.^{11,12,16,17} Therefore, in order to begin to test whether the inactivation of D₂ and D₃ receptors affects the normal neurochemical phenotype of the striatum, the present study utilized these three markers to analyse and compare their expression in the striatum of adult wild-type mice and mice deficient for D₂ and D₃ receptors.

EXPERIMENTAL PROCEDURES

Animals

Mice deficient for the DA D₂ and D₃ receptor were generated by gene targeting via homologous recombination.¹³ The homozygous mutants and their wild-type littermates used in the present study have a hybrid 129Sv×C57Bl/6 genetic background. D₂/D₃ double mutants were generated by cross-breeding homozygous D₃ females with homozygous D₂ males. Heterozygous double mutants were interbred and the resulting offspring included wild-type and homozygous double mutants which occurred with the expected Mendelian frequency of one in 16. Animals were housed under a constant 12-h/12-h light–dark cycle with free access to food and water. Male mice at postnatal day 60 were used. A total of seven animals per genetic group (wild-type, D₂ and D₃ single mutants, and D₂/D₃ double mutants) was analysed in this study. All experimental procedures were carried out in accordance with the National Institutes of Health Guide for the Care and Use of Laboratory Animals, and all efforts were made to limit the number of animals used in this study.

Tissue preparation

Animals were deeply anesthetized with xylazine (10 mg/kg, i.p.) and ketamine (30 mg/kg, i.p.), and perfused transcardially with 1% cold paraformaldehyde/phosphate-buffered saline (PBS) for 1 min, followed by perfusion with 4% paraformaldehyde/PBS for 9 min. Brains were then quickly removed and postfixed in 4% paraformaldehyde/PBS for 6 h at 4°C. To achieve cryoprotection, brains were equilibrated in 30% sucrose/PBS for two days at 4°C, frozen on dry ice and stored at –80°C. Tissues were cut coronally at 40 µm using a freezing microtome. Six consecutive sections of five series (each comprising 15 tissue sections) of the region containing the dorsal striatum were processed and stored at 4°C in PBS/1% sodium azide.

Immunocytochemistry

Tissue sections were incubated in PBS supplemented with 5% normal horse serum, 5% crystallized bovine serum albumin and 2% gelatin. For TH immunostaining, 0.3% Triton X-100 was added to the incubation buffer. Tissue sections were incubated with a mouse monoclonal anti-TH/immunoglobulin G (IgG) antibody (dilution 1:4000; Incstar, Stillwater, MN, U.S.A.) at 4°C for two days. Calbindin immunoreactivity was detected after incubating tissue sections with a mouse monoclonal anti-CB antibody (dilution 1:6000; SWant, Bellinzona, Switzerland) at 4°C for three days. After incubation with primary antibody, sections were washed with PBS (three times for 10 min) and incubated with a biotinylated horse anti-mouse IgG secondary antibody (dilution 1:500; Vector Laboratories, Burlingame, CA, U.S.A.) for 90 min at room temperature. After rinsing with PBS, sections were incubated with PBS containing 0.5% bovine serum albumin and an avidin–peroxidase complex (Vectastain ABC kit, Vector Laboratories) for another 90 min at room temperature. Sections were developed with 0.05% 3,3'-diaminobenzidine, mounted on to gelatinized slides, air-dried, defatted in a 1:1 mixture of 95% ethanol and formaldehyde, and dehydrated in ethanol. Xylene-equilibrated sections were mounted using DPX mounting medium and examined with bright-field microscopy. Additional sections were rehydrated and counterstained with Cresyl Violet to clarify the cytoarchitecture.

For the analysis of CB immunoreactivity with fluorescence microscopy,

sections were immersed in a fluorescein isothiocyanate-conjugated goat anti-mouse IgG secondary antibody (dilution 1:200; Vector Laboratories) for 2 h at room temperature, washed in PBS, mounted on to gelatinized slides, air-dried and coverslipped with Vectorshield mounting medium (Vector Laboratories). For double-labeling experiments, postfixed sections (4% paraformaldehyde and 0.15% glutaraldehyde) were incubated simultaneously with the mouse monoclonal anti-CB antibody (dilution 1:3000) and a rabbit polyclonal anti-GABA antibody (dilution 1:2000; Sigma, St Louis, MO, U.S.A.). After a three-day incubation at 4°C, sections were washed in PBS, incubated for 2 h at room temperature with both a fluorescein isothiocyanate-conjugated anti-mouse IgG (dilution 1:200) and a Texas Red-conjugated anti-rabbit IgG (dilution 1:200) secondary antibody (Vector Laboratories), and processed as described above. Sections were analysed using a confocal laser scanning microscope (Zeiss LSM 410; Zeiss, Oberkochen, Germany) equipped with ×16 and ×40 Zeiss Plan-Neofluar objectives.

Acetylcholinesterase histochemistry

AChE activity was analysed using a histochemical protocol described elsewhere.²³ In brief, sections were incubated in 30 µM iso-N,N'-bis(1-methylethyl)pyrophosphorodiamidic anhydride/0.2 M Tris–maleate (pH 5.7) for 30 min at room temperature, followed by a 30-min dark incubation in an AChE solution containing 130 mM Tris–maleate (pH 5.7), 5 mM sodium citrate, 3 mM cupric sulfate, 0.5 mM potassium ferricyanide and 25 mg/50 ml of acetylthiocholine iodide. Sections were rinsed with PBS, mounted on to gelatinized slides, air-dried and dehydrated. Xylene-equilibrated sections were mounted with DPX mounting medium and examined with bright-field microscopy.

Immunoblotting and reverse transcriptase–polymerase chain reaction analysis

For the analysis of the expression levels of TH immunoreactivity, proteins were extracted in a buffer containing 1×PBS, 1% Nonidet P-40, 0.5% sodium deoxycholate and 0.1% sodium dodecyl sulfate supplemented with 2 mM sodium vanadate (Na₃VO₄), 20 mM sodium fluoride, 1 mM EGTA, 1 mM dithiothreitol, 1 µM microcystin and protease inhibitors. The protein concentration in each lysate was determined using the BCA protein assay kit (Pierce, Rockford, IL, U.S.A.). A mouse monoclonal anti-TH antibody (Incstar, Stillwater, MN, U.S.A.; dilution 1:10,000) was used to probe Immobilon polyvinylidene fluoride membrane (Millipore, Bedford, MA, U.S.A.) blots of sodium dodecyl sulfate–polyacrylamide gel electrophoresis gels, which contained 50 µg of total protein in each lane. Bound antigen was visualized using a peroxidase-conjugated goat anti-mouse IgG secondary antibody (Kirkegaard & Perry Laboratories, Gaithersburg, MD, U.S.A.) in conjunction with enhanced chemiluminescence (ECL; Pierce).

For reverse transcriptase–polymerase chain reaction (RT–PCR) experiments, total cytoplasmic RNA was extracted from dorsal striatal tissues using the guanidine/cesium chloride ultracentrifugation method. First-strand cDNA was synthesized from 10 µg of total RNA using an oligo-dT₁₅ primer in conjunction with 200 units of Moloney Murine Leukemia Virus reverse transcriptase (United States Biochemical, Cleveland, OH, U.S.A.). In exponential RT–PCR experiments, the amino terminal 480 nucleotides of the open reading frame of the dopamine transporter (DAT) cRNA was amplified using the primer pair DAT5': 5'-ATGAGTAAGCAAAATGCTCC-3' and DAT3': 5'-GATGATGACATTGTAGAA-3', and equal aliquots of the first strand cDNA reaction. For PCR amplifications from templates of each genotype, five PCR tubes containing equal aliquots of one PCR mastermix were taken to different endpoints (10, 15, 20, 25 and 30 cycles of amplification). The respective PCR products were analysed on Southern blots probed with a ³²P-radiolabeled, cDNA-encoding mouse DAT.

RESULTS

Expression of calbindin-D_{28k} in the striatum

A distinct expression pattern of the calcium-binding protein CB characterizes the neurochemical differentiation of the developing and mature striatum.^{16,17} The heterogeneously distributed CB immunoreactivity is confined to the striatal

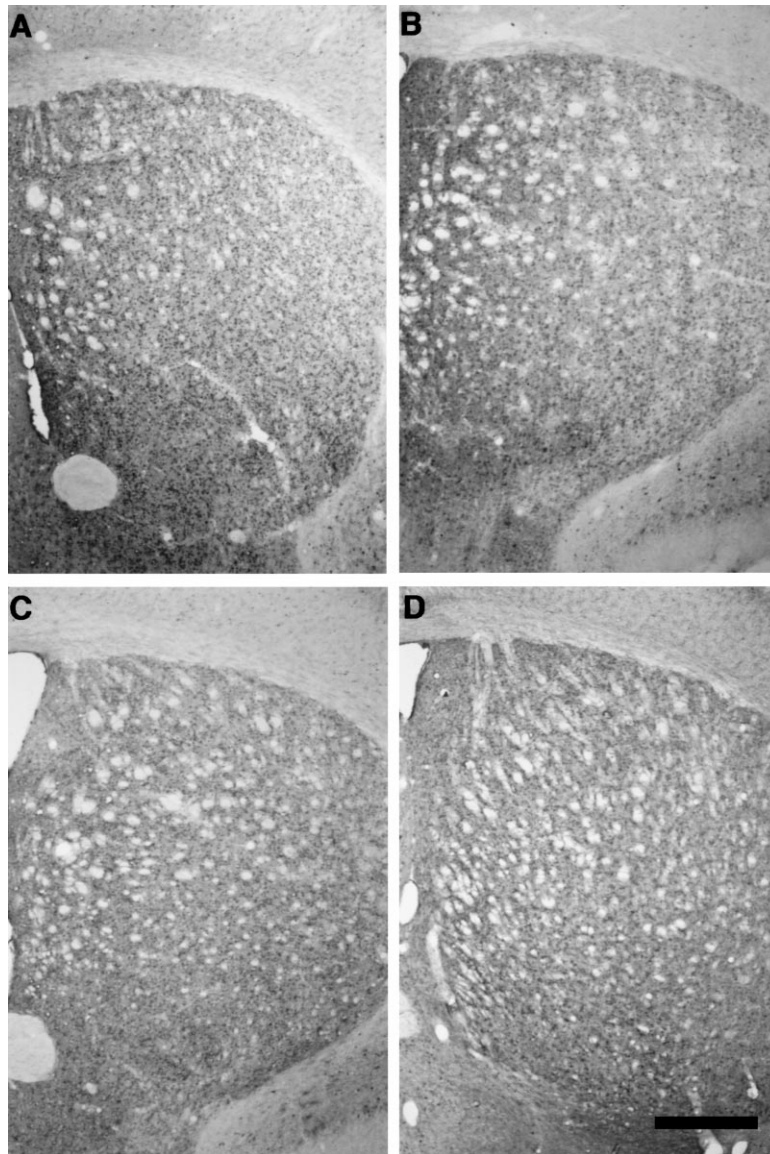


Fig. 1. Distribution of CB immunoreactivity in the striatum of wild-type (A), D₂ mutant (B), D₃ mutant (C) and D₂/D₃ double mutant (D) mice at postnatal day 60 (P60). Note the higher intensity of CB immunoreactivity in the neuropil of the ventromedial part compared to the dorsolateral part of the striatum in the wild-type and D₂ mutant animals. This ventromedial–dorsolateral gradient in staining intensity is less apparent in the D₃ mutant or the D₂/D₃ double mutant mice that are characterized by a more homogeneous immunostaining pattern. Scale bar = 500 μ m.

matrix compartment, where it is concentrated within the medium-sized spiny neurons (the principal projection neurons of the neostriatum), and their projecting axons terminating in the globus pallidus, entopeduncular nucleus and substantia nigra; the major subcellular compartment of CB expression is the matrix of the cytoplasm of these cells.^{8,10} The following experiments used an antibody raised against CB to identify CB-containing neurons in the dorsal striatum of D₂ and D₃ receptor mutant mice and their wild-type littermates. A first series of experiments employed light microscopy to determine the topography of expression of CB immunoreactivity. The results are shown in Fig. 1. In wild-type mice, a dense CB immunoreactivity is found in the ventromedial region of the striatum and a lesser density of CB-immunoreactive neuropil is detected dorsolaterally (Fig. 1A). This result is consistent with previous findings of a gradient of CB immunoreactivity in the rat, which is strongest in the ventral and medial parts and lowest in the dorsolateral parts of the caudate–putamen.¹⁷

The topography of striatal CB expression of D₂ single mutant is indistinguishable from wild-type (Fig. 1B). However, the cellular pattern of CB expression differs substantially between wild-type and D₂ single mutants. As shown in Fig. 2A and C, in medium spiny neurons of wild-type animals, CB immunoreactivity is prominent in the nucleus and the cytoplasm. Interestingly, whereas the nuclei of wild-type animals are the most intensely labeled cellular structures (Fig. 2C), the nuclei of many CB-containing neurons of D₂ single mutants show no CB staining (Fig. 2B, D). The cytoplasmic CB staining, however, as well the staining of proximal dendrites of CB-positive neurons are very similar between wild-type (Fig. 2A, C) and D₂ mutants (see Fig. 2B, D).

A complementary analysis of CB-immunostained material by confocal laser scanning microscopy further illustrates the different cellular distribution of CB immunoreactivity in D₂ single mutants. These results are shown in Fig. 3. In wild-type mice, CB immunoreactivity is distributed homogeneously

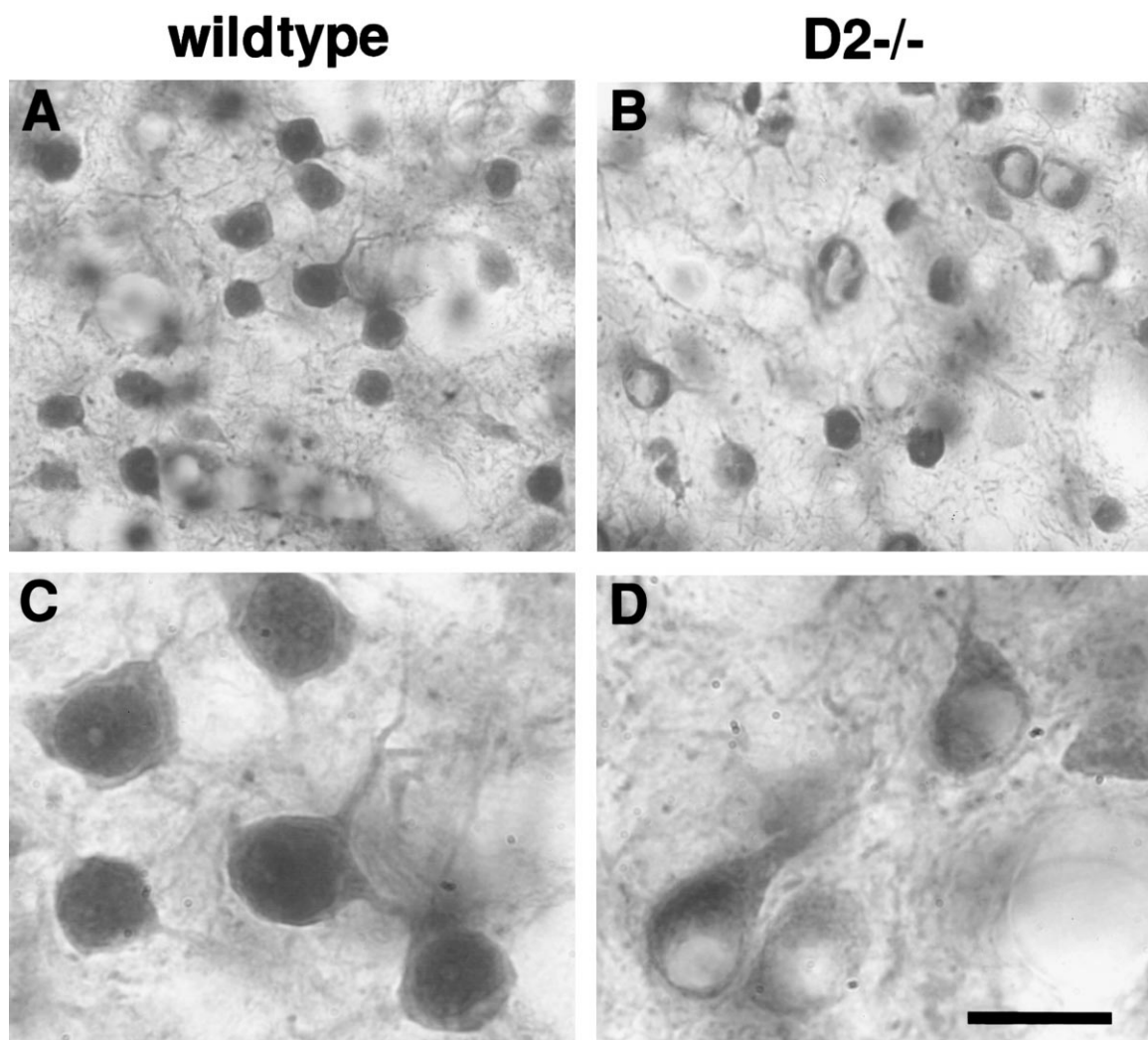


Fig. 2. Cellular patterns of CB immunoreactivity in the ventromedial part of the striatum in a wild-type (A, C) and a D_2 mutant (B, D). CB immunolabeling is prominent in the nuclei and the cytoplasm of medium spiny neurons in the wild-type animal, where the nuclei are the most intensely labeled structures (see high magnification in C). In contrast, the D_2 mutant shows virtually no nuclear labeling in these neurons (B, D), while the cytoplasmic staining is comparable to that in the wild-type mice (compare C and D). Scale bar = 25 μm (D; also applies to C), 50 μm (A, B).

throughout the cell body and does not spare the nucleus (Fig. 3A). In contrast, CB-immunoreactive neurons of D_2 single mutants are highly concentrated in the cytoplasmic rim, where they also appear to form distinct clusters of particularly dense CB immunoreactivity. The nuclei of these CB-positive neurons, however, are not labeled (Fig. 3B). As shown further in Fig. 3D, similar alterations in the cellular distribution of CB immunoreactivity are also detected in D_2/D_3 double mutants (Fig. 3D).

In contrast to results obtained with D_2 single and D_2/D_3 double mutants, the cellular distribution of CB immunoreactivity of D_3 single mutants is indistinguishable from wild type (Fig. 3A, C). However, as shown in Fig. 1, the ventromedial–dorsolateral gradient of expression of striatal CB immunoreactivity seen in wild-type and D_2 single mutants (Fig. 1A, B) is less apparent in D_3 single mutants and D_2/D_3 double mutants (Fig. 1C, D). The most obvious change in the density of CB labeling is detected in a region corresponding to the core and shell of the nucleus accumbens, which displayed intense CB labeling with a much denser immunoreactivity in the neuropil of wild-type compared to D_3 mutants (Fig. 1A, C). Thus, in D_3 single mutants, the most apparent difference in

the topography of CB expression is found in a region of the striatum that, in the adult brain, is known to express D_3 receptors at high levels.⁶

The observations made above raise the question of whether there is a change in the types of neurons that express CB. To begin to test this, additional striatal sections were double-labeled for CB and the neurotransmitter GABA, and processed for fluorescence microscopy (see Experimental Procedures). However, the experiment revealed no obvious change in the types of neurons that express CB immunoreactivity. As shown in Fig. 4A and B, the majority of CB-immunoreactive neurons of wild-type mice is GABAergic neurons and only a few neurons are non-GABAergic. Similarly, CB-immunoreactive cells of all three mutants are mostly GABAergic and only a few non-GABAergic neurons were found to express CB (Fig. 4C–H). Consistent with the results shown in Fig. 1, the sections shown in Fig. 4 illustrate that the density of CB immunoreactivity in the dorsolateral neuropil of the striatum of D_3 mutants and D_2/D_3 double mutants is very similar to the corresponding density found ventromedially (Fig. 4E–H). In sections of wild-type and D_2 mutants, however, the density of CB-immunoreactive

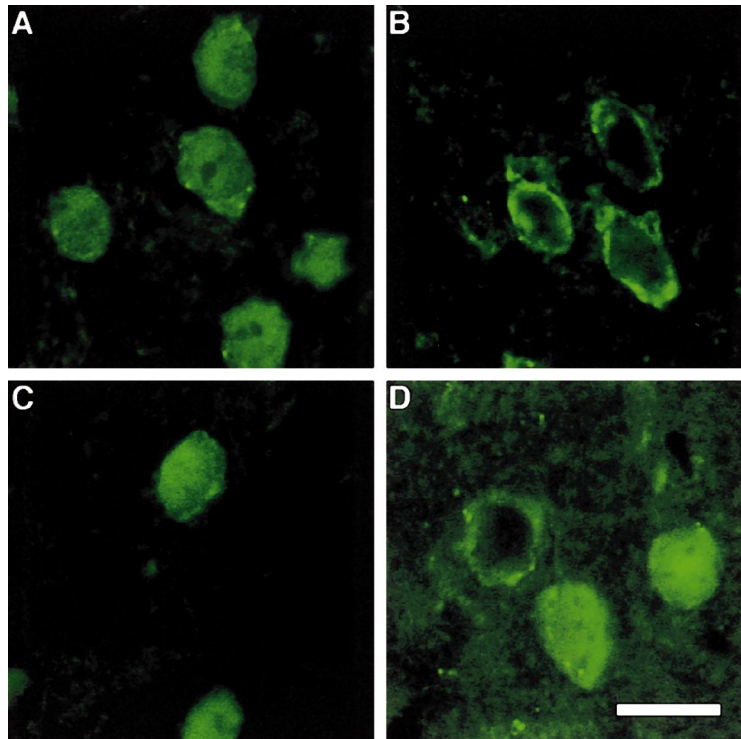


Fig. 3. Confocal laser scanning microscopy analysis of the cellular localization of CB in wild-type (A), D₂ mutant (B), D₃ mutant (C) and D₂/D₃ double mutant (D) mice. Wild-type and D₃ mutant mice display a homogeneous labeling throughout the cytoplasm and nucleus, whereas in the D₂ mutant CB immunoreactivity is restricted to a rim of cytoplasm and spares the nucleus. An intermediate pattern is observed in the D₂/D₃ double mutant. Scale bar = 15 μ m.

neuropil in the ventromedial region appears to be slightly higher than the corresponding density detected dorsolaterally (Fig. 4A–D).

In summary, mice lacking D₂ receptors show an altered cellular distribution of CB immunoreactivity that is not detected in mice lacking D₃ receptors. Mice lacking D₃ receptors express less CB immunoreactivity in the core and shell region of the nucleus accumbens and the typical ventromedial–dorsolateral gradient of expression of striatal CB is less apparent. Mice lacking D₂ and D₃ receptors show a combination of both phenotypes.

Expression of tyrosine hydroxylase immunoreactivity and acetylcholinesterase activity in the dorsal striatum

Although the mature dorsal striatum contains the highest concentration of D₂ receptors and also expresses D₃ receptors,¹⁸ Nissl-stained sections obtained from the striatum of adult mutants that developed in the absence of D₂ and D₃ receptors (i.e. D₂ and D₃ single mutants and D₂/D₃ double mutants) revealed that the general anatomy appears normal (not shown). However, the results shown above revealed distinct alterations in the expression of CB in adult mutants, indicating that the lack of D₂-like receptors has receptor subtype-specific consequences for the expression of one neurochemical phenotype of the striatal matrix. These results motivated the following experiments that tested whether two other neurochemical phenotypes of the mature striatum, namely the expression of TH and AChE, may be altered in mice lacking D₂ and D₃ receptors.

As shown in Fig. 5, the expression of TH immunoreactivity is indistinguishable between wild-type, D₂ and D₃ single mutants, and D₂/D₃ double mutants. The diffuse TH staining

throughout the dorsal striatum seen in animals of all four genotypes at postnatal day 60 is characteristic of the mature striatum.¹² Furthermore, as shown in Fig. 6A, total levels of striatal TH immunoreactivity detected on immunoblots of proteins extracted from the dorsal striatum are also indistinguishable between wild-type and the various mutants. Additional experiments employed exponential RT–PCR experiments to analyse the striatal expression levels of mRNA encoding the DAT. As shown in Fig. 6B, neither the reduction of expression of both D₂ and D₃ receptors (heterozygous double mutants) nor the complete absence of both receptors in homozygous double mutants alters the expression levels of DAT mRNA (Fig. 2B).

The data shown in Figs 5 and 6, together with our previous findings of normal tissue levels of striatal DA,¹³ indicate that the dense dopaminergic innervation of the striatum is unaltered in mice that develop without D₂ and/or D₃ receptors. Moreover, as shown in Fig. 7, a histochemical method employed to localize AChE in the dorsal striatum of wild-type (Fig. 7A) and mutant mice (Fig. 7B–D) revealed a mature histochemical staining pattern of AChE^{11,12} in all four genotypes which is characterized by an abundant expression of AChE throughout the striatum, where AChE-poor islands (striosomes) are well delineated from AChE-rich areas (matrix) that surround them.

Altogether, in contrast to the alterations in the expression of striatal CB, the expression of TH immunoreactivity and AChE is unaffected in the striatum of adult mice deficient for D₂ and D₃ receptors.

DISCUSSION

To test whether the constitutive lack of DA D₂ and D₃

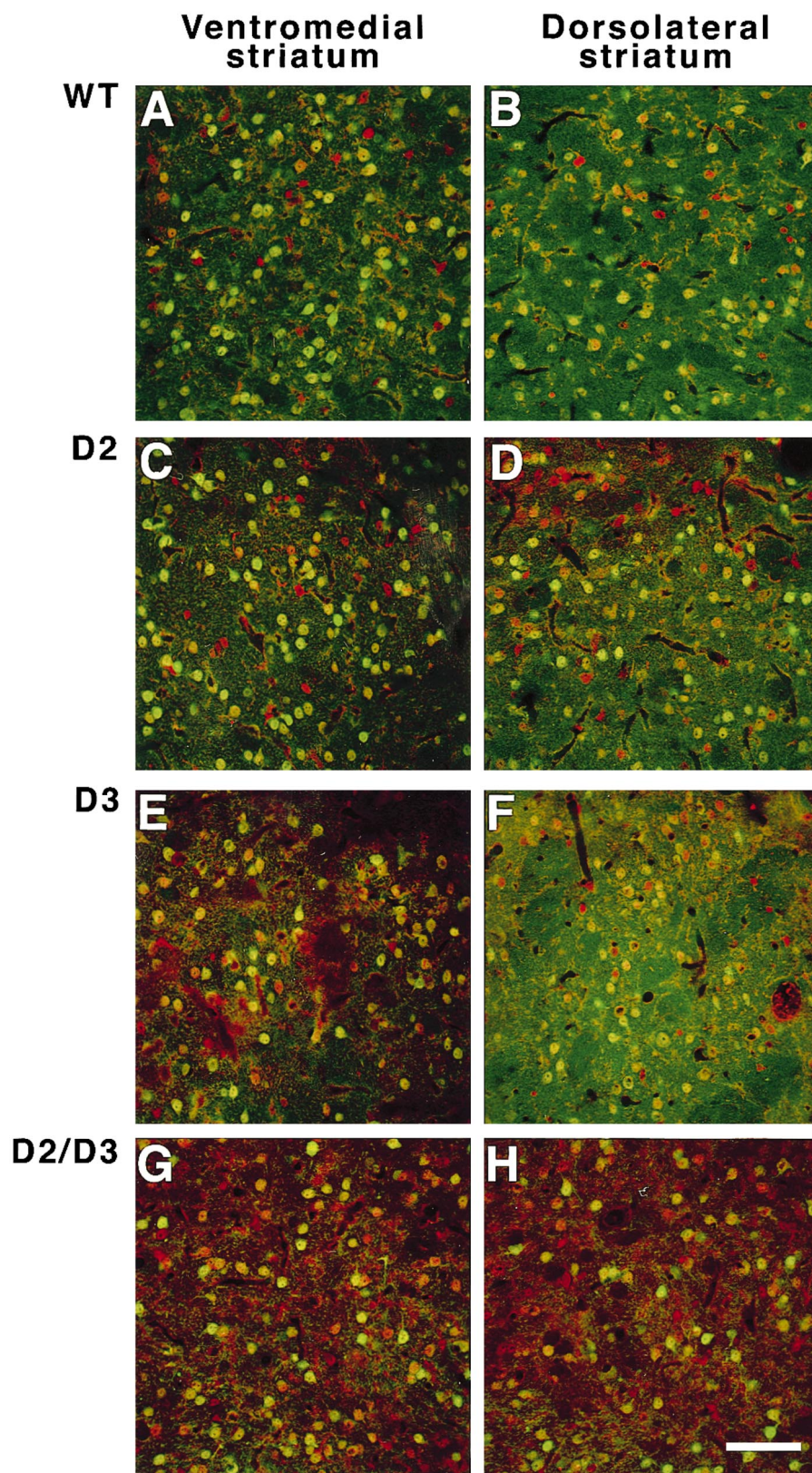


Fig. 4. Confocal laser scanning microscopy analysis of the localization of CB (green fluorescence) and GABA (red fluorescence) in the ventromedial striatum (left column) and dorsolateral striatum (right column) of wild-type (A, B), D₂ mutant (C, D), D₃ mutant (E, F) and D₂/D₃ double mutant (G, H) mice. There is a slightly higher density of CB-immunoreactive neurons in the ventromedial part of the striatum in wild-type and D₂ mutant mice, compared to the dorsolateral part (A–D). The densities of CB-immunoreactive neurons are roughly comparable in the D₃ mutant and D₂/D₃ double mutant mice (E, F). In all cases only a few GABAergic neurons did not express CB. Scale bar = 100 μ m.

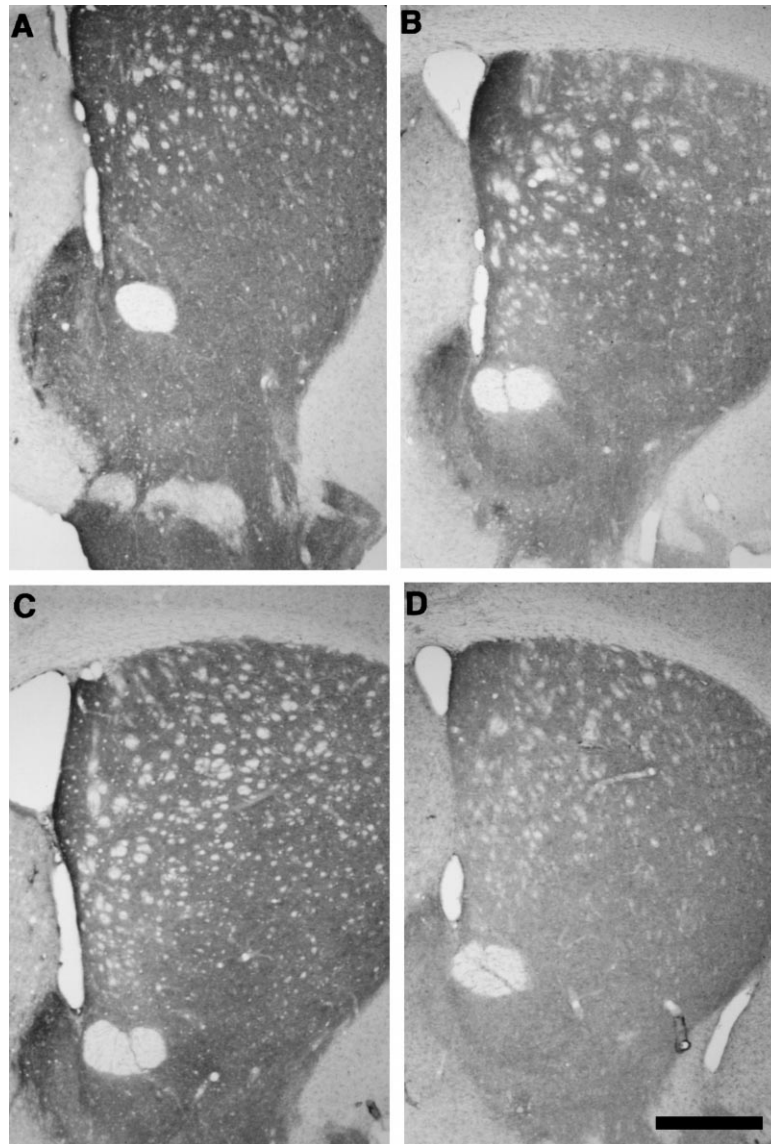


Fig. 5. Distribution of TH immunoreactivity in the striatum of postnatal day 60 (P60) wild-type (A), D₂ mutant (B), D₃ mutant (C) and D₂/D₃ double mutant (D) mice. Note the homogeneous staining pattern in all four animals. Scale bar = 500 μm.

receptor expression affects the neurochemical differentiation of the striatum, the present study analysed the expression of three neurochemical markers, TH, AChE and CB, in striatal tissue of adult mice deficient for DA D₂ and D₃ receptors. The

distinct expression patterns of these three markers are well documented, and they characterize both the developing and the mature dorsal striatum.^{11,12,16,17}

A main finding of the present study is an altered cellular

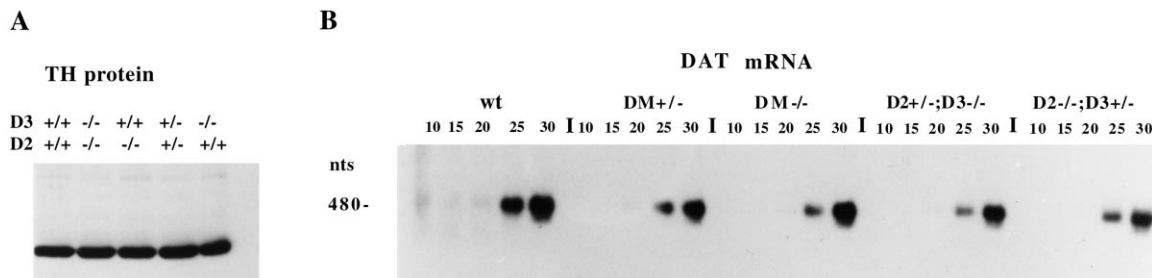


Fig. 6. Expression of TH immunoreactivity (A) and DAT mRNA (B) in the dorsal striatum. The levels of TH in 50 μg of total cellular dorsal striatal protein (detected with a monoclonal anti-TH antibody) are indistinguishable between wild-type, D₂ and D₃ single mutants, and heterozygous and homozygous double mutants. The expression of the low abundant DAT mRNA was analysed by exponential RT-PCR. On Southern blots of PCR products obtained from RNA templates of wild-type and the four genetic combinations of D₂/D₃ double mutants, the earliest time-point of detection of DAT mRNA is after 25 cycles of RT-PCR amplification, indicating no significant change in the expression of DAT mRNA in the double mutants. DM -/-, homozygous double mutants; DM +/-, heterozygous double mutants.

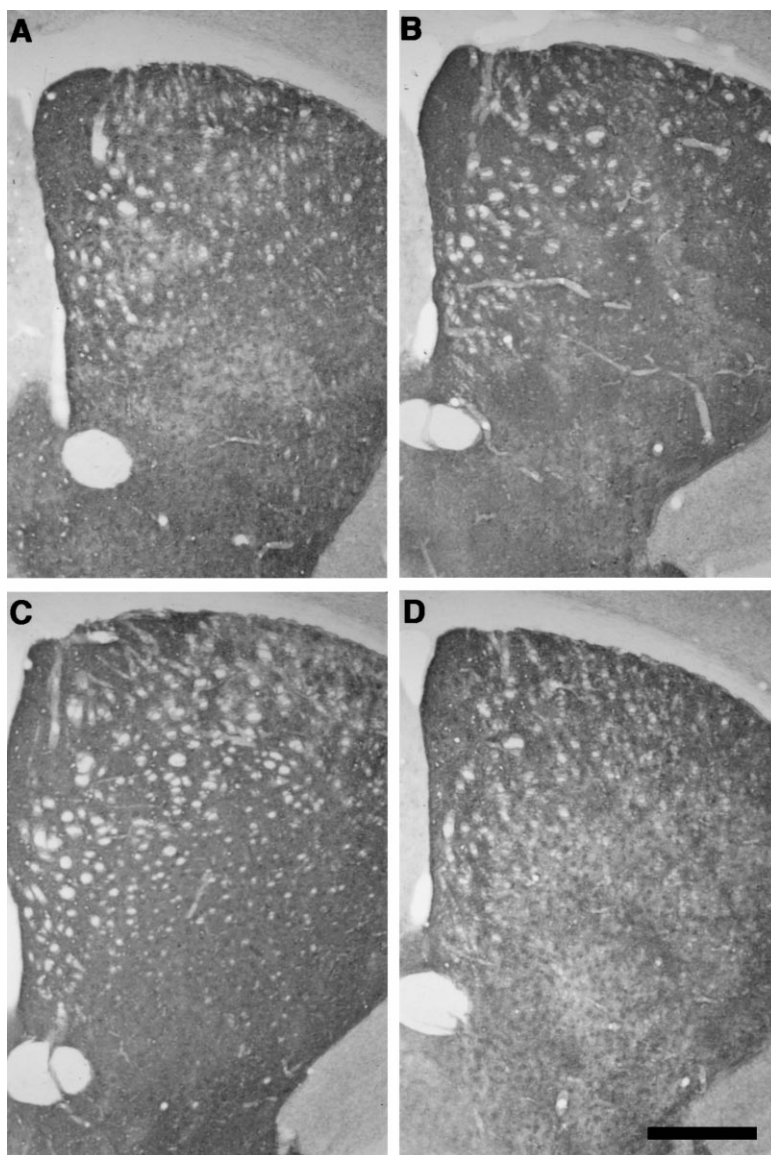


Fig. 7. Distribution of AChE in the striatum of wild-type (A), D_2 mutant (B), D_3 mutant (C) and D_2/D_3 double mutant (D) mice at postnatal day 60 (P60). AChE activity differentiates the AChE-rich striatal matrix from the AChE-poor striosomal compartment, and this pattern is also visible in D_2 and D_3 single mutants and in the D_2/D_3 double mutant. Scale bar = 500 μm .

distribution of CB in D_2 , but not in D_3 , mutant mice. In striatal neurons of wild-type mice, CB immunoreactivity is prominently expressed in both the nucleus and the cytoplasm of striatal medium spiny neurons. In fact, the most intensely labeled structures are the nuclei of these neurons. In D_2 mutants, however, CB immunoreactivity is highly concentrated in the cytoplasmic rim. Both the light microscopic analysis of 3,3'-diaminobenzidine-stained sections (Fig. 2) and the analysis of CB-immunostained sections by confocal laser scanning microscopy (Fig. 3) illustrate a virtually complete absence CB expression in the nucleus of affected neurons of D_2 mutants. This change in the cellular distribution of CB immunoreactivity is likely to have functional consequences. The calcium-binding protein CB is expressed at high concentration and binds Ca^{2+} with high affinity. The role of CB is therefore thought to be largely that of an intracellular buffer.⁴ The distinct change in the cellular distribution of CB in striatal neurons of D_2 mutants would therefore indicate that virtually all of the Ca^{2+} -buffering capacity of CB

is concentrated in the cytoplasm. Moreover, the almost exclusive concentration of CB in the cytoplasmic rim of striatal neurons of D_2 mutants, as well as the distinct clustering of CB immunoreactivity detected therein (see Fig. 3B), suggest a close proximity of CB and the cell membrane. A direct demonstration of the possible association of CB with the cell membrane (or even membrane channels), however, requires the further analysis of immunostained sections by electron microscopy. Such future studies, combined with electrophysiological studies, could then test one compelling hypothesis, namely that the distinct cellular distribution of CB in neurons of D_2 mutants increases the buffering capacity for Ca^{2+} entering through voltage-sensitive Ca^{2+} or *N*-methyl-D-aspartate channels, either to protect cells that have lost D_2 receptors against the damaging effects of excessive Ca^{2+} influx during prolonged periods of high activity⁴ or to modulate rising intracellular Ca^{2+} signals that are critical for the establishment of synaptic plasticity which, in the striatum of D_2 mutants, has been shown to be altered.⁵ In any case, the

reason why the cellular distribution of CB is altered in striatal neurons of D₂ mutants will only become apparent when the functional consequences of this altered cellular expression of CB are elucidated. (Note that a number of different functional properties has been attributed to CB.^{2,14,19}) Moreover, as shown in Fig. 2, many, but not all, neurons of the striatum of D₂ mutants show the altered cellular expression pattern of CB, suggesting that this phenotype is perhaps limited to the population of neurons that would normally express D₂ receptors (a possibility that, in the genetic null mutants studied here,¹³ could only be tested indirectly with, for example, CB/enkephalin double-labeling experiments).

Despite the different cellular distribution pattern, the striatal topography of CB expression is similar in wild-type and D₂ single mutants. In both genotypes, the lesser density of CB-immunoreactive neuropil in the dorsolateral region of the striatum appears to reflect the normal ventromedial–dorsolateral gradient of CB expression that is maintained throughout the development of the striatum.^{16,17} It is, however, noted in Fig. 1 that D₃ mutants (which show a wild-type-like cellular distribution pattern of CB) express less CB immunoreactivity in the ventral striatum, a region corresponding to the nucleus accumbens, in which D₃ receptors are expressed at highest levels in the adult brain.¹⁵ As a result, the ventromedial–dorsolateral gradient of CB expression is less apparent in these mutants. This observation, together with the fact that the D₃ receptor itself shows a ventral to dorsal expression gradient,⁶ suggest the possibility that D₃ receptors promote the expression of CB. However, a more robust evaluation of the significance of the observation made in the present study requires a future detailed quantitative assessment that involves a rigorous stereological estimate of changes, based on a well-defined set of criteria, to analyse subregional changes of CB expression and its correlation with D₃ receptor expression levels. The present study could only begin to ask whether the changes in CB expression seen in D₃ mutants are due to changes in the types of neurons that express CB. It is known that most of the striatal CB-expressing neurons are GABAergic neurons and, despite the alterations in CB expression seen in D₂ and D₃ mutants, we found that this is still the case for all four genotypes tested here (Fig. 4). Thus, further studies will have to test whether substance P/dynorphin- and enkephalin-expressing neurons, or, more generally, neurons

that are part of the striatopallidal and striatonigral system, are affected to a similar or different extent.

The changes in the expression of CB immunoreactivity described above are not paralleled by changes in the expression of two other markers that characterize the neurochemical differentiation of the striatum. Our results indicate a normal dopaminergic innervation of the dorsal striatum of mice lacking D₂ and D₃ receptors. Results from immunocytochemical and immunoblotting experiments revealed that the expression of striatal TH immunoreactivity is unaffected. Furthermore, mRNA encoding the DAT is expressed at normal levels. Moreover, our previous study has shown that the tissue levels of striatal DA are indistinguishable between wild-type and D₂/D₃ mutants.¹³ Similar results were obtained with mice lacking DA D₁ receptors,²⁴ indicating that the lack of neither of the two most abundant DA receptors expressed in the striatum (D₁ and D₂ receptors) affects the development of a dense dopaminergic innervation of the striatum. Moreover, neither the absence of D₁ receptors nor the absence of D₂ and D₃ receptors affects, respectively, the appearance of striatal interneurons²⁴ and the expression of AChE (present study).

CONCLUSIONS

The present study revealed an altered cellular distribution but a normal topography of expression of CB in mice lacking D₂ receptors. In D₃ mutants, the cellular distribution of CB is indistinguishable from wild-type. In these mutants, however, a decreased density of CB-immunoreactive neuropil was found in a region of the ventral striatum that is known to express highest levels of D₃ receptors. Mice lacking both D₂ and D₃ receptors show a combination of the D₂ and D₃ mutant phenotypes. The different and mutant-specific alterations in the expression pattern detected for CB (but not TH or AChE) may contribute to the different locomotor phenotypes seen in the two types of mutants.

Acknowledgements—We thank W. G. M. Janssen for help with the confocal imaging, and G. Yeung and A. P. Leonard for technical assistance. This work was supported by National Science Foundation Grant IBN-9808567 (C.S.) and National Institutes of Health Grant MH51623 (C.S.).

REFERENCES

- Accili D., Fishburn C. S., Drago J., Steiner H., Lachowicz J. E., Park B.-H., Gauda E. B., Lee E. J., Cool M. H., Sibley D. R., Gerfen C. R., Westphal H. and Fuchs S. (1996) A targeted mutation of the D3 dopamine receptor gene is associated with hyperactivity in mice. *Proc. natn. Acad. Sci. U.S.A.* **93**, 1945–1949.
- Airaksinen M. S., Eilers J., Garaschuk O., Thoenen H., Konnerth A. and Meyer M. (1997) Ataxia and altered dendritic calcium signaling in mice carrying a targeted null mutation of the calbindin D28K gene. *Proc. natn. Acad. Sci. U.S.A.* **94**, 1488–1493.
- Baik J.-H., Picetti R., Dalardi A., Thirlet G., Dierich A., Depaulis A., Le Meur M. and Borelli E. (1995) Parkinsonian-like locomotor impairment in mice lacking dopamine D2 receptors. *Nature* **377**, 424–428.
- Baimbridge K. G., Celio M. R. and Rogers J. H. (1992) Calcium-binding proteins in the nervous system. *Trends Neurosci.* **15**, 303–308.
- Calabresi P., Saiardi A., Pisani A., Baik J.-H., Centonze D., Mercuri N. B., Bernadi G. and Borrelli E. (1997) Abnormal synaptic plasticity in the striatum of mice lacking dopamine D2 receptors. *J. Neurosci.* **17**, 4536–4544.
- Demotes-Mainard J., Henry C., Jeantet Y., Arsaut J. and Arnauld E. (1996) Postnatal ontogeny of dopamine D3 receptors in the mouse brain: autoradiographic evidence for a transient cortical expression. *Devl Brain Res.* **94**, 166–174.
- Diaz J., Ridray S., Mignon V., Griffon N., Schwartz J.-C. and Sokoloff P. (1997) Selective expression of dopamine D3 receptor mRNA in proliferative zones during embryonic development of the rat brain. *J. Neurosci.* **17**, 4282–4292.
- DiFiglia M., Christakos S. and Aronin N. (1989) Ultrastructural localization of immunoreactive calbindin-D28K in the rat and monkey basal ganglia, including subcellular distribution within colloidal gold labeling. *J. comp. Neurol.* **279**, 653–665.
- Drago J., Gerfen C. R., Lachowicz J. E., Steiner H., Hollon T. R., Love P. E., Ooi G. T., Grinberg A., Lee E. J., Huang S. P., Bartlett P. F., Jose P. A., Sibley D. R. and Westphal H. (1994) Altered striatal function in a mutant mouse lacking D1A dopamine receptors. *Proc. natn. Acad. Sci. U.S.A.* **91**, 12,564–12,568.
- Gerfen C. R., Baimbridge K. G. and Miller J. J. (1985) The neostriatal mosaic: compartmental distribution of calcium-binding protein and parvalbumin in the basal ganglia of the rat and monkey. *Proc. natn. Acad. Sci. U.S.A.* **82**, 8780–8784.

11. Graybiel A. M., Pickel V. M., Joh T. H., Reis D. J. and Ragsdale C. W., Jr (1981) Direct demonstration of a correspondence between the dopamine islands and acetylcholinesterase patches in the developing striatum. *Proc. natn. Acad. Sci. U.S.A.* **78**, 5871–5875.
12. Graybiel A. M. (1984) Correspondence between the dopamine islands and striosomes of the mammalian striatum. *Neuroscience* **13**, 1157–1187.
13. Jung M.-Y., Skryabin B. V., Arai M., Abbondanzo S., Fu D., Brosius J., Robakis N. K., Polites H. G., Pinter J. E. and Schmauss C. (1999) Potentiation of the D2-mutant motor phenotype in mice lacking dopamine D2 and D3 receptors. *Neuroscience* **91**, 911–924.
14. Köhr G., Lambert C. E. and Mody I. (1991) Calbindin-D28K (CaBP) levels and calcium currents in acutely dissociated epileptic neurons. *Expl Brain Res.* **85**, 543–551.
15. Levant B. (1997) The D3 dopamine receptor: neurobiology and potential clinical relevance. *Pharmac. Rev.* **49**, 231–252.
16. Liu F.-C. and Graybiel A. M. (1992) Transient calbindin-D28K-positive systems in the telencephalon: ganglionic eminence, developing striatum and cerebral cortex. *J. Neurosci.* **12**, 674–690.
17. Liu F.-C. and Graybiel A. M. (1992) Heterogeneous development of calbindin-D28K expression in the striatal matrix. *J. comp. Neurol.* **320**, 304–322.
18. Missale C., Nash S. R., Robinson S. W., Jaber M. and Caron M. G. (1998) Dopamine receptors: from structure to function. *Physiol. Rev.* **78**, 189–225.
19. Nägerl U. V. and Mody I. (1998) Calcium-dependent inactivation of high-threshold calcium currents in human dentate gyrus granule cells. *J. Physiol.* **509**, 39–45.
20. Sales N., Martres M. P., Bouthenet M. L. and Schwartz J.-C. (1988) Ontogeny of dopaminergic D₂ receptors in the rat nervous system: characterization and detailed autoradiographic mapping with [¹²⁵I]iodosulpiride. *Neuroscience* **28**, 673–700.
21. Schambra U. B., Duncan G. E., Breese G. R., Fornaretto M. G., Caron M. G. and Fremeau R. T., Jr (1994) Ontogeny of D1A and D2 dopamine receptor subtypes in rat brain using *in situ* hybridization and receptor binding. *Neuroscience* **62**, 65–85.
22. Sibley D. R. (1999) New insight into dopaminergic receptor function using antisense and genetically altered animals. *A. Rev. Pharmac. Toxic.* **39**, 313–341.
23. Woolf N. J. and Butcher L. L. (1981) Cholinergic neurons in the caudate–putamen complex proper are intrinsically organized: a combined Evans Blue and acetylcholinesterase analysis. *Brain Res. Bull.* **7**, 487–507.
24. Xu M., Moratalla R., Gold L. H., Hiroi N., Koob G. F., Graybiel A. M. and Tonegawa S. (1994) Dopamine D1 receptor mutant mice are deficient in striatal expression of dynorphin and in dopamine-mediated behavioral responses. *Cell* **79**, 729–742.
25. Xu M., Koeltzow T. E., Santiago G. T., Moratalla R., Cooper D. C., Hu X.-T., White N. M., Graybiel A. M., White F. J. and Tonegawa S. (1997) Dopamine D3 receptor mutant mice exhibit increased behavioral sensitivity to concurrent stimulation of D1 and D2 receptors. *Neuron* **19**, 837–848.

(Accepted 18 January 2000)